PAPER

Methanol conversion on ZSM-22, ZSM-35 and ZSM-5 zeolites: effects of 10-membered ring zeolite structures on methylcyclopentenyl cations and dual cycle mechanism†

Mozhi Zhang,‡[ad] Shutao Xu,‡[a] Yingxu Wei,*[a] Jinzhe Li,[a] Jingrun Chen,[a] Jinbang Wang,[a] Wenna Zhang,[ad] Shushu Gao,[ad] Xiujie Li,[b] Congxin Wang[b] and Zhongmin Liu*[ac]

ZSM-22, ZSM-35 and ZSM-5, aluminosilicate zeolites possessing 10-membered ring channels, have been used in the present study as the catalysts of the MTO reaction. The diversities in dimensions and connection types of the 10-membered ring channels of the three zeolite catalysts make their performances in the MTO reaction quite different. As the key active species involved in the hydrocarbon-pool mechanism in the MTO reaction, methylcyclopentenyl cations (MCP$^+$) and methylbenzenes have been captured by ^{13}C MAS NMR and GC-MS over the three zeolite catalysts during methanol conversion. The comparative studies of the retained organics generation over the zeolite catalysts indicate that due to the spatial confinement effects of the inorganic frameworks, the retained organic species generated in the catalysts during the MTO reaction are influenced by both their sizes and amounts. A detailed analysis of the confined organic species showed the formation of MCP with varied methyl substitutions over the three zeolites. ^{12}C/^{13}C-methanol switch experiments were employed to investigate the reaction route for product generation. The differences in the participation levels of the methylbenzene and methylcyclopentadiene over the three zeolite catalysts imply that the formation and function of the organic species formed in the 10-membered ring channel were impacted by the chemical environment of the zeolites, and the methanol conversion that occurred in the 10-membered ring channels of the three zeolites also followed different reaction routes.

1. Introduction

Over the past 30 years, since the methanol to olefin (MTO) reaction was first discovered and investigated by Chang *et al.*,[1,2] the MTO process has been developed as an alternative route to olefin production from naphtha cracking.[3,4] Starting from coal, by using the MTO technology, the production of light olefins *via* a non-petrochemical route has been realized.[5,6]

[a]*National Engineering Laboratory for Methanol to Olefins, Dalian National Laboratory for Clean Energy, iChEM (Collaborative Innovation Center of Chemistry for Energy Materials), Dalian Institute of Chemical Physics, Chinese Academy of Sciences, Dalian 116023, P. R. China. E-mail: liuzm@dicp.ac.cn; weiyx@dicp.ac.cn; Fax: +86 411 84691570; Tel: +86 411 84379335*

[b]*Dalian National Laboratory for Clean Energy, Dalian Institute of Chemical Physics, Chinese Academy of Sciences, Dalian 116023, P. R. China*

[c]*State Key Laboratory of Catalysis, Dalian Institute of Chemical Physics, Chinese Academy of Sciences, Dalian 116023, P. R. China*

[d]*University of Chinese Academy of Sciences, Beijing 100039, P. R. China*

† Electronic supplementary information (ESI) available. See DOI: 10.1039/c6ra08884h

‡ Both authors contributed equally to this work.

In terms of fundamental research on the MTO process, there have been more than 20 reaction mechanisms proposed to depict the conversion of methanol and generation of olefin products.[7–11] Among them, the direct formation mechanisms of C–C bonds from methanol or dimethyl ether (DME) for product generation were theoretically proved unfavourable, due to the high energy barriers in these routes.[3,12–14] The hydrocarbon-pool mechanism, an indirect way to generate olefins, proposed by Dahl *et al.*, has achieved more and more support.[15–17] This indirect method avoids the high energy barriers in computational simulation and was successfully proved by accumulating evidence in experiments.[4,12,18]

Among the catalysts with different topologies, ZSM-5, with MFI topology, has been regarded as the important candidate for the MTO and MTG (methanol to gasoline) processes, due to its distinct selectivity for olefin and aromatic product generation.[1,2,19] Intensified research has been focused on the investigation of the mechanism of the ZSM-5-catalyzed MTH reaction.[20–26] In 2006, when performing the ^{12}C/^{13}C-methanol switch experiments, Svelle *et al.* found the inconsistence of ethene and higher alkenes in ^{13}C content and proposed that the

formation of ethene is mechanistically different from higher alkenes on ZSM-5.[27] The dual cycle mechanism was then put forward, as being made up of the aromatic cycle and alkene cycle, and used to illuminate many phenomena in the MTH reaction.[28] Some works have exhibited the various tendencies of the dual cycle mechanism in methanol conversion on different zeolites.[29–36]

In the aromatic cycle, methylbenzenium cations, methyl-cyclopentenyl cations and the deprotonated hydrocarbons have been proved to behave as the reaction intermediates during methanol conversion.[20,37–39] Haw et al. detected alkyl-substituted cyclopentenyl cations on zeolites with the help of solid-state magic-angle-spin (MAS) NMR and considered alkyl-substituted cyclopentenyl cations as active species in the MTH reaction on ZSM-5 zeolites.[20,22,40] Methylcyclopentenyl cations (MCP^+) are important active intermediates in the MTO reaction, and have been captured in the methanol conversion catalyzed by several different kinds of zeolites, such as ZSM-5, SSZ-13, SAPO-34, beta and ZSM-22.[20,38,41–43] Wang et al. also observed several larger alkyl-substituted cyclopentenyl cations in the work of the MTH reaction on ZSM-5.[44–47]

The formation of the above-mentioned carbenium cations, as active intermediates in the MTH reaction, depends significantly on the chemical environment of the zeolite. The confinement effect of the zeolite inorganic framework on the size or structure of the active intermediates is an important characteristic of zeolite-catalyzed MTH reactions.[48–54] With cage dimensions of 1.27×0.94 nm, SAPO-34, or SSZ-13, can accommodate relatively large organic species in the MTH reaction, even pyrene. Hexamethylbenzene (hexaMB), the heptamethylbenzenium cation ($heptaMB^+$) and the pentamethylcyclopentenyl cation ($pentaMCP^+$) are confirmed as active intermediates in SAPO-34 or SSZ-13.[38,41,55,56] Although the space in beta, made up of intercrossing 12-membered ring channels, is a little smaller than the cage of SAPO-34, the main active intermediates are similar.[37,42,57] However, when the space continues to be reduced to the size of the intersections of 10-membered ring channels like ZSM-5, hexaMB, $heptaMB^+$ and $pentaMCP^+$ are then too large to be generated and work efficiently. Instead, the lower methyl-substituted 5- or 6-membered cycle species, such as the pentamethylbenzenium cation ($pentaMB^+$), dimethylcyclopentenyl cation ($diMCP^+$) and trimethylcyclopentenyl cation ($triMCP^+$) tend to be active intermediates in ZSM-5.[20,39,44,45] The confinement effects of the zeolite structure on active intermediates are apparently different among SAPO-34, beta and ZSM-5. Sometimes, even a slight variation in the zeolite structure can bring great discrepancy in reaction performance.[49,52,58–60] ZSM-12 and ZSM-22 are both made up of one-dimensional, straight, 10-membered ring channels with MTW and TON topologies, respectively. The difference between the diameter of ZSM-12 channels and that of ZSM-22 is only 0.3 Å, but ZSM-12 shows much more methanol conversion than that on ZSM-22. Both the experimental analysis and theoretical simulation show that the cyclic species, polymethylbenzene, can be generated and the aromatic cycle and the alkene cycle can both proceed actively on ZSM-12, but on ZSM-22, it is difficult to achieve the aromatic cycle because of the limited space; only the alkene cycle mechanism occurs. The difference of 0.3 Å in the diameter of the channels causes dramatic changes in reaction mechanism and performance.[58,59]

Both the structures of ZSM-22 and ZSM-5 zeolites are built up by channels of 10-membered rings. ZSM-22 is a one-dimensional straight channel zeolite, while ZSM-5 is a three-dimensional channel zeolite containing two types of inter-connecting channels: straight channels (5.6×5.3 Å) and sinusoidal channels (5.5×5.1 Å), which can provide a wider space than the space of the straight channels of the 10-membered rings in ZSM-22. The MTO performances between ZSM-22 and ZSM-5 are also quite different, as well as their mechanisms. The MTO reaction on ZSM-22 mainly goes through alkene methylation and cracking, and on ZSM-5, the reaction follows the dual cycle mechanism.[53,61,62] One of our previous studies showed that alkyl-substituted cyclopentenyl cations could also be captured on the ZSM-22 zeolite by solid-state MAS NMR in the MTH reaction, and ZSM-22 zeolites could also convert methanol by the aromatic cycle, as well as the alkene cycle,[43] which more or less present the reaction route of the dual cycle mechanism.[27,28]

In the present study, besides ZSM-5 and ZSM-22, the ZSM-35 zeolite with FER topology, possesses a two-dimensional interconnecting channel system: the 10-membered ring channel of 5.4×4.2 Å, perpendicular to the 8-membered ring channel of 4.8×3.5 Å, was also introduced as the catalyst for methanol conversion.[63] The investigation of the methanol reaction over these 10-membered ring zeolites aims to clarify the reaction intermediate formation and function over the three catalysts with slight structural differences and correlate the channel connecting structure to the particularity of the reaction route over each catalyst.

2. Experimental

2.1 Catalysts

The KZSM-22 catalyst was supplied by Group DNL0802 of the Dalian Institute of Chemical Physics, Dalian, China, and synthesized according to the method developed by Kokotailo et al.[64] The organic template was removed by calcination at 600 °C for 10 h in air. The HZSM-22 was obtained through ion-exchange with 1.0 mol L^{-1} NH_4NO_3 aqueous solution at 80 °C, followed by calcination at 550 °C for 4 h.[43,65,66]

Zeolite ZSM-35 was synthesized from the reaction mixture having the batch molar composition of 2.5 Na_2O : 1.0 Al_2O_3 : 35 SiO_2 : 9.0 cyclohexylamine : 750 H_2O, prepared by admixing silica sol (25.59 wt% SiO_2, 0.31 wt% Na_2O, 74.1 wt% H_2O, Qingdao Haiyang Chemical Co., Ltd.), sodium aluminate solution (16.9 wt% Al_2O_3, 24.2 wt% Na_2O, homemade), sodium hydroxide (96 wt% NaOH, Shenyang Chemical Reagent factory), cyclohexamine (99.5 wt%, Tianjin Bodi Chemicals Co., Ltd.) and deionized water. The synthesis gel was stirred for 2 h at room temperature before being transferred into a 100 mL stainless-steel autoclave. Then, it was subjected to hydrothermal treatment at 160 °C for 48 h in an oven under autogenous pressure, while being rotated at 30 rpm. After the hydrothermal treatment, the product was recovered by filtration, washed

thoroughly with hot distilled water, and dried at 120 °C. The organic template was removed by calcination at 520 °C for 4 h in air. The H-form of ZSM-35 was obtained through ion-exchange with 0.5 mol L^{-1} NH$_4$NO$_3$ solution at 80 °C for 2 h (1 g of ZSM-35 in 10 mL of solution), followed by calcination at 520 °C for 2 h; the ion-exchange process was repeated thrice.[67,68]

HZSM-5 was the commercial product, NKF-5 zeolite, from the Catalyst Plant of Nankai University.

The Si/Al ratios of the three obtained H-type zeolites of ZSM-22, ZSM-35 and ZSM-5 are 31.7, 14.3 and 17.9, respectively.

2.2 Catalyst characterization

The powder XRD patterns of the three H-type zeolites were recorded on a PANalytical X'Pert PRO X-ray diffractometer with Cu-Kα (λ = 1.5418 Å) at 40 kV and 40 mA. The chemical composition was measured by a Philips Magix-601 X-ray fluorescence (XRF) spectrometer. The crystal size and morphology were determined by field emission scanning electron microscopy (FE-SEM, Hitachi, SU8020). N$_2$ adsorption and desorption experiments were carried out on a Micromeritics ASAP 2020 physical adsorption analyzer at 77 K.[69]

The ^{1}H, ^{29}Si, ^{27}Al and ^{13}C MAS NMR spectra of zeolites were recorded on a Bruker Avance III 600 spectrometer with a 14.1 T wide-bore magnet, using a 4 mm MAS probe, and respective resonance frequencies were 600.13, 119.2, 156.4 and 150.9 MHz. Before the ^{1}H MAS NMR experiment, the samples were typically dehydrated at 673 K and a pressure below 10^{-3} Pa for 20 h. ^{1}H MAS NMR spectra were recorded using a single pulse sequence with a π/4 pulse of 2 μs and a 10 s recycle delay, with adamantane (1.74 ppm) as the chemical shift reference. All samples were weighed for the quantification of Brönsted acid density, and their ^{1}H MAS NMR spectra were resolved by Dmfit software with Gaussian–Lorentz line shapes, using adamantane (1.74 ppm) as the quantitative external standard, measured under the same NMR acquisition conditions.[42,70,29] Si MAS NMR spectra were recorded with a spinning rate of 6 kHz using high-power proton decoupling. 1024 scans were accumulated with a π/4 pulse width of 2.5 μs and a 10 s recycle delay. Chemical shifts were referenced to 4,4-dimethyl-4-silapentane sulfonate sodium salt (DSS) at 0 ppm. ^{27}Al MAS NMR experiments were performed with a spinning rate of 12 kHz using a one pulse sequence. 600 scans were accumulated with a π/8 pulse width of 0.75 μs and a 2 s recycle delay. Chemical shifts were referenced to (NH$_4$)Al(SO$_4$)$_2$·12H$_2$O at −0.4 ppm. ^{13}C MAS NMR spectra were recorded using high-power proton decoupling with a spinning rate of 12 kHz. 2048 scans were accumulated with a π/4 pulse width of 1.8 μs and a 4 s recycle delay. The chemical shifts were referenced to adamantane with the upfield methine peak at 29.5 ppm.[42]

2.3 Methanol-to-hydrocarbon conversion

The catalysts were pressed and sieved to particles in 40–60 mesh and loaded into a microscale fixed-bed stainless steel tubular reactor with an inner diameter of 5 mm. Before the reaction, the catalysts were activated at 500 °C in a N$_2$ flow of 25 mL min^{-1} for 40 min. Then, the temperature of the reactor was adjusted to 300 °C for methanol conversion. All of the reactions were performed under atmospheric pressure. Methanol was fed by passing the carrier gas through a saturator containing methanol to give a weight hourly space velocity (WHSV) of 2 h^{-1}. The effluent products from the reactor were kept warm and analyzed by an online gas chromatograph (GC) equipped with a PoraPLOT-Q capillary column, an FID detector and a mass spectrometric detector (Agilent 7890B/5977A). The conversion and selectivity were calculated on a CH$_2$ basis. Dimethyl ether (DME) was considered as a reactant in the calculation.

The confined organics in the catalyst during methanol conversion were measured by ^{13}C solid-state NMR, following the procedure mentioned above and employing ^{13}C-methanol as the reactant. ^{13}C-methanol was fed into the reactor for 20 min with the WHSV of 2 h^{-1} and then the reactor was quickly immersed and quenched by liquid nitrogen to stop the reaction and the cooled catalyst was discharged and transferred into an NMR rotor in the glove box without exposure to ambient air.

2.4 ^{12}C/^{13}C-methanol switch experiments

In the ^{12}C/^{13}C-methanol switch experiments, after ^{12}C-methanol was fed for 20 min, it was stopped and the feeding line was switched to ^{13}C-methanol for a further 0.5–2 min. The isotopic distributions of effluents were also analyzed by online GC-MS (Agilent 7890B/5977A) in Section 2.3. After the reaction, the reactor was quickly quenched with liquid nitrogen to stop the reaction and the catalysts were discharged for analysis as described in Section 2.5.

2.5 Confined organics determination with GC-MS

After the reaction, the catalyst was quickly cooled down, transferred into a Teflon vial and dissolved in 20% (wt) HF solution for 1 h. After completely dissolving the catalyst, CH$_2$Cl$_2$ was added to the vessel and the retained species in the catalyst was extracted. Before separating the mixture, KOH solution was used to neutralize the excessive amount of acid. Then, the CH$_2$Cl$_2$-extracted organic phase was analyzed by GC-MS (Agilent 7890A/5975C) equipped with a HP-5 capillary column, an FID detector and a mass spectrometric detector.[34,71] Hexachloroethane was used as the internal standard, and the mass spectral library used here was NIST11.

3. Results and discussion

3.1 Description of catalyst topologies

Three kinds of aluminosilicate zeolites, ZSM-22, ZSM-35 and ZSM-5, with 10-membered ring channel systems are illustrated in Fig. 1, and channel dimensions and channel sizes are summarized in Table 1.

From Table 1 and Fig. 1, ZSM-22 only has a one-dimensional, straight 10-membered ring channel with a size of 5.7 × 4.6 Å. ZSM-35 has a two-dimensional textural structure and a 10-membered ring channel of 5.4 × 4.2 Å, perpendicular to the 8-membered ring channel of 4.8 × 3.5 Å. The intersection of the two-dimensional channels provides a large space, and the maximum diameter of a sphere that can be included is 6.31 Å,
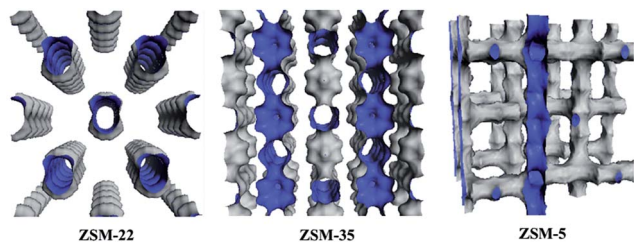
Fig. 1 Illustrations of the channel systems of ZSM-22, ZSM-35 and ZSM-5.

larger than that in ZSM-22. ZSM-5 has a three-dimensional crosslinking network structure. Perpendicular to the plane of the two-dimensional 10-membered ring sinusoidal channel, there is another straight, 10-membered ring channel passing through the plane and intercrossing with the sinusoidal channel. The intersections of these 10-membered ring channels, with sizes of 5.6 × 5.3 Å and 5.5 × 5.1 Å, respectively, are slightly larger than those in ZSM-35 and the maximum diameter of a sphere that can be included is 6.36 Å.

The three zeolites studied in the present work can be viewed as a series of catalysts with very similar 10-membered ring channels, but are different in their dimensionalities and interconnections.

3.2 Catalyst characterization

The powder XRD patterns (Fig. S1†) show the high purity and crystallinity of the three zeolite catalysts, HZSM-22, HZSM-35 and HZSM-5. SEM images (Fig. S2†) of the three samples manifest the morphologies and sizes of the crystal grains. XRF measurement provides the chemical composition. The framework Si/Al ratios of the samples (Table 1) were calculated by deconvolutions of the ^{29}Si MAS NMR spectra (Fig. S3†), according to the Loewenstein's rule[72] and the values are very close to that obtained by measurement of XRF. ^{27}Al MAS NMR spectra (Fig. S4†) show that most of the Al atoms are in the tetrahedral coordination state as the framework aluminum. BET surface areas and Brönsted acid densities were determined from N$_2$ adsorption isotherms in Fig. S5 and ^{1}H MAS NMR

spectra in Fig. S6,† respectively. The characterization results are listed in Table 1.

3.3 Catalytic performances of the MTH reaction

Fig. 2 demonstrates the effluent product distribution of the MTH reaction on ZSM-22, ZSM-35 and ZSM-5 at the reaction temperature of 300 °C and methanol WHSV of 2 h^{-1}. Methanol conversions on all the three zeolite catalysts present the character of the induction period under the reaction condition of low temperature. In the early reaction period, at time on stream (TOS) of 5 min, the methanol conversion on the three zeolites are all quite low, lower than 1%, which can be attributed to the slow kinetics in the induction period. When the reaction time reaches 20 min, the reaction activities of the three catalysts are all improved and methanol conversion reaches the highest value during the entire test. After that, the reaction activities tend to get lower and lower and the hydrocarbon product generation is decreased in the subsequent reaction time.

Though the variation tendencies of reactions on the three catalysts are quite similar, the methanol conversion and selectivities of hydrocarbon products show big differences. The MTH
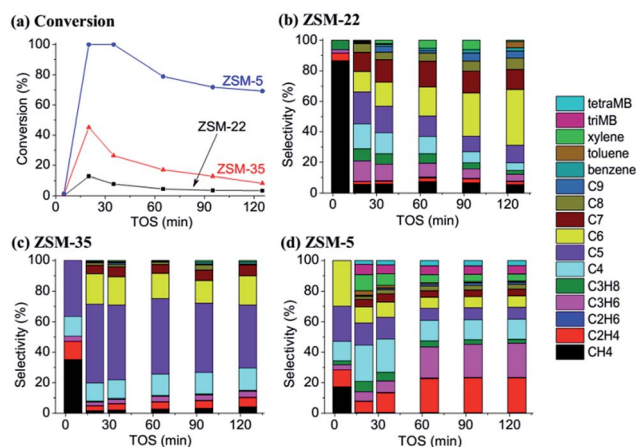

Fig. 2 Conversion and product distribution of MTH reactions over ZSM-22, ZSM-35 and ZSM-5 at reaction temperature of 300 °C and methanol WHSV of 2 h^{-1}.

Table 1 Description of the 10-membered ring channel aluminosilicate zeolites, ZSM-22, ZSM-35 and ZSM-5, investigated in this study according to data in the structure database of the international zeolite association (IZA), and characterization results

		10-Membered ring channel system								
Sample	Topology	Dimension	Channel size	Maximum diameter of a sphere that can be included	Morphology[a]	Size[a]	Si/Al[b]	Framework Si/Al[c]	BET surface area[d]	Brönsted acid density[e]
ZSM-22	TON	1	5.7 × 4.6 Å	5.71 Å	Rod-like	0.2 μm	31.7	31.3	216 m^2 g^{-1}	0.58 mmol g^{-1}
ZSM-35	FER	2	5.4 × 4.2 Å 4.8 × 3.5 Å	6.31 Å	Flake	0.4 μm	14.3	19.4	328 m^2 g^{-1}	0.76 mmol g^{-1}
ZSM-5	MFI	3	5.6 × 5.3 Å 5.5 × 5.1 Å	6.36 Å	Hexagonal	1.5 μm	17.9	19.0	355 m^2 g^{-1}	0.77 mmol g^{-1}

^{a} Data from SEM. ^{b} Data from XRF. ^{c} Data from ^{29}Si MAS NMR. ^{d} Data from N$_2$ adsorption. ^{e} Data from ^{1}H MAS NMR.

activity of ZSM-22 is the lowest of the three catalysts, and the maximum methanol conversion is only 13% at time on stream of 20 min. ZSM-35 displays a slightly higher conversion, up to 45%. As an industrialized MTH catalyst, ZSM-5 presents the highest methanol conversion among the three catalysts, with the maximum conversion of 100%. The methanol conversion level and the selectivities of the hydrocarbon products differ greatly. Comparing the effluent product distribution at the respective highest conversions (Fig. 3), almost all the products of the MTH reactions on ZSM-22 and ZSM-35 are chain alkenes, mainly C_3–C_7, but there is a small difference in the distribution. On ZSM-22, the C_3–C_7 hydrocarbons are almost evenly distributed and each component takes on more than 20%. On ZSM-35, the distribution of the C_3–C_7 hydrocarbons is more concentrated, with C_5 olefins alone accounting for nearly 50% and C_4–C_6 hydrocarbons taking up more than 80%. On ZSM-5, the effluents are quite different. Apart from chain olefins, there are a number of alkanes and aromatics generated, mainly isobutane, isopentane and xylene. Compared to ZSM-22 and ZSM-35, ethene is predominantly formed over ZSM-5, compared to the other two zeolites.

Olefins generation from methanol conversion over 10-membered ring zeolites may follow a dual cycle reaction mechanism: the aromatic cycle with the involvement of active aromatic compounds as the hydrocarbon-pool species, and the alkene cycle, with alkene generation from the reaction of the alkene methylation and cracking route.[27,28] As mentioned in section 3.1, ZSM-22 is made up of one-dimensional channels, and the narrow space of the 10-membered ring channel strongly restricts the growth of organic species, and chain olefins are mainly produced. For ZSM-35, the orthogonally intersectional 10-membered ring channel and 8-membered ring channel create a little larger space than the isolated 10-membered ring channel, and the similar alkene product generation over ZSM-35 implies that the methanol conversion may also follow the alkene methylation and cracking route as that over ZSM-22. However, on ZSM-5, three-dimensional 10-membered ring interconnecting channels allow the generation of larger cyclic species, which may initiate aromatic cycle mechanism and greatly improve the methanol conversion.[20,53,73] All these three zeolites possess 10-membered ring channels, but the methanol conversion and effluent product distribution imply that the differences in connecting types of the 10-membered ring channels in these zeolites may vary the detailed reaction route of methanol reaction.

3.4 ^{13}C MAS NMR and GC-MS study of retained species and carbenium ion formation

The MTH reaction is an auto-catalysis reaction, and the organic species formed and retained in the zeolite or the generated effluent alkene products are considered as co-catalysts for methanol conversion.[7,74] In Section 3.3, the effluent product distributions have been determined. Whether the organic species retained in the zeolite participate in the olefin generation is undoubtedly very important for the MTH reaction. Analysis of the organic species retained in the catalyst is usually helpful to clarify the reaction mechanism.

Without destroying the catalyst, ^{13}C MAS NMR spectroscopy has advantages in the detection of retained species in zeolites.[75–77] Fig. 4 shows the ^{13}C MAS NMR spectra of the quenched catalysts, ZSM-22, ZSM-35 and ZSM-5, from MTH reactions at TOS of 20 min. The signals representing aromatics (130–140 ppm) and methylcyclopentenyl cations (MCP$^+$, 240–260 ppm and ~150 ppm) appear in the spectra of all three catalysts, even the benzenium cation (207 ppm and 191 ppm) is captured on ZSM-5. The great difference in the signal intensity of these retained species on the three zeolites is worth noting. In the spectra of ZSM-22 and ZSM-35, the strongest signals are from dimethyl ether (DME) and methanol, which is consistent
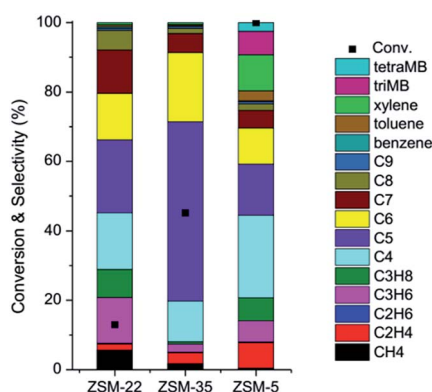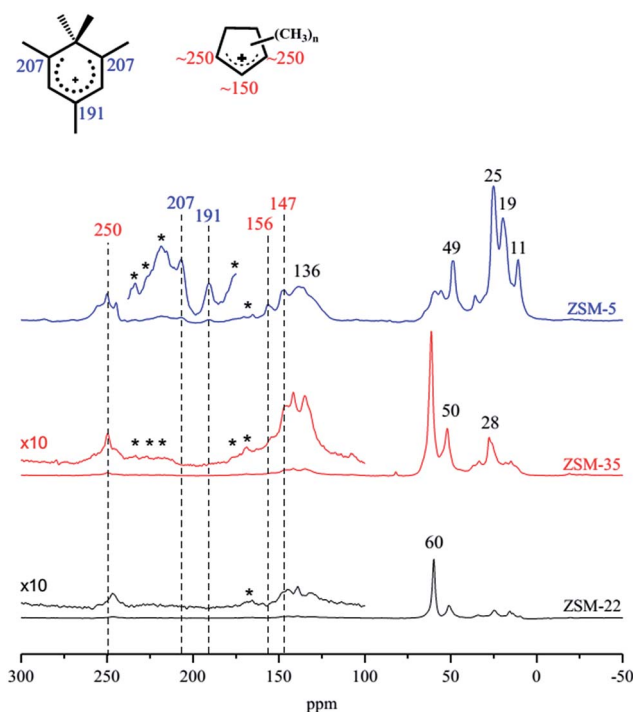

Fig. 3 Effluent distribution of MTO products at the respective highest conversion at TOS of 20 min over ZSM-22, ZSM-35 and ZSM-5 at reaction temperature of 300 °C and methanol WHSV of 2 h^{-1}.

Fig. 4 ^{13}C MAS NMR spectra of retained species at the respective highest conversions over ZSM-22, ZSM-35 and ZSM-5 at reaction temperature of 300 °C and methanol WHSV of 2 h^{-1}.

with the large amount of unreacted methanol among the effluents. Very weak peaks at ~250 ppm, ~136 ppm and ~25 ppm are detected, which means only a small amount of cyclic organic species is retained in the ZSM-22 catalyst during the reaction. These observations for ZSM-22 also appear in the spectra of ZSM-35, with merely a slight increase in the intensity of the cyclic organics. For ZSM-5, the signals of aromatics and cyclopentenyl cations appear at very high intensity, compared to those in ZSM-22 and ZSM-35, indicating that much more organic species were formed and retained in ZSM-5 than in the other two zeolites.

ZSM-5 manifests excellent MTH reaction activity with the formation and deposition of large amounts of organic species in the catalyst. On the contrary, ZSM-22 and ZSM-35 show much lower methanol conversion and at the same time, the detected retained organic species are of very low intensity. A positive correlation is suspected for the MTH reaction activity with the amount of retained organic species in ZSM-22, ZSM-35 and ZSM-5 under these reaction conditions.

Additionally, the retained organic species (TOS = 20 min) in zeolites were also analyzed by GC-MS after dissolving the catalyst in HF solution and extracting the organics in CH_2Cl_2 solution (Fig. 5(a)). Similar to ^{13}C MAS NMR results, the organic species retained in the catalysts are composed of aromatics and methylcyclopentadienes (MCP, deprotonated products of methylcyclopentenyl cations, and the deprotonation process from MCP^+ to MCP is shown in Scheme S1†), and the amount of cyclic organics detected in ZSM-5 is much higher than those in ZSM-22 and ZSM-35.

In MTH reactions, the organic species retained in the catalyst are usually confined by the fine structure of the zeolite, and their sizes and structures are related to the chemical environment of the zeolites.[37,49,51,52,58–60] Though ZSM-22, ZSM-35 and ZSM-5 all possess 10-membered ring channels, different arrangements of channels cause various intersections and space, which have great influence on the generation of retained organics.

Methylcyclopentenyl cations were captured in ZSM-5 by Haw et al. and Wang et al.,[20,44,45] and in our very recent study, cyclopentenyl cations were also found in ZSM-22 during methanol conversion.[43] In these studies, cyclopentenyl cations are proved to be active intermediates in MTH reactions over ZSM-5 and ZSM-22. However, the specific cyclopentenyl cations on ZSM-22 and ZSM-5 are different in the number or size of the alkyl substitution groups. From the GC-MS analysis of the retained species in ZSM-22, ZSM-35 and ZSM-5 catalysts after methanol conversion in Fig. 5(a), several ion chromatograms of the organics with m/z = 94, 108, 122, 136, respectively, representing dimethylcyclopentadienes (diMCP), trimethylcyclopentadienes (triMCP), tetramethylcyclopentadienes (tetraMCP) and pentamethylcyclopentadienes (pentaMCP) or their isomers, are extracted and shown in Fig. 5(b)–(d). After integration and normalization of the peaks with a certain m/z value, the distributions of various cyclopentadienes in three zeolites are obtained (Fig. 5(e)). Comparing the formed MCP distribution, methylcyclopentadienes on ZSM-5 mainly have 3, 4 and 5 methyl substitution (m/z = 108, 122, 136), while 2 and 3 methyl-
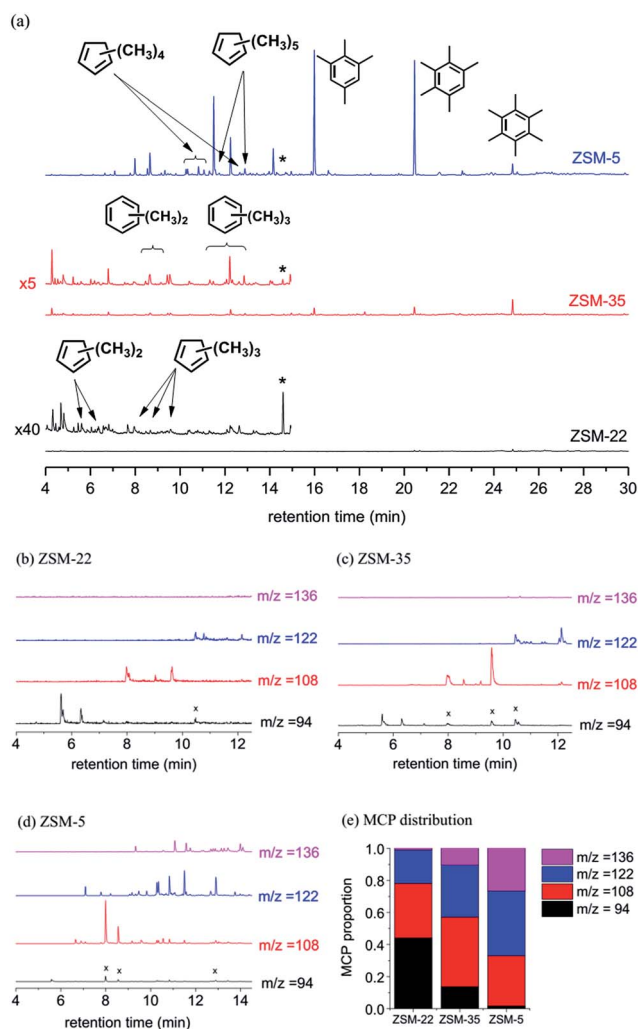

Fig. 5 GC–MS analysis of the extracted organics retained in zeolites after methanol conversion for 20 min at reaction temperature of 300 °C and methanol WHSV of 2 h^{-1}. (a) shows the chromatographic analysis of the three samples, * denotes internal standard C_2Cl_6; (b), (c) and (d) are extracted ion chromatograms (EIC) over ZSM-22, ZSM-35 and ZSM-5, respectively, X denotes the peaks of fragment ions from heavier MCP; (e) is the distribution of methylpentadienes (MCP) with different methyl group substitutions in ZSM-22, ZSM-35 and ZSM-5 zeolites. m/z = 94, 108, 122, 136, respectively, representing dimethylcyclopentadienes (diMCP), trimethylcyclopentadienes (triMCP), tetramethylcyclopenta-dienes (tetraMCP) and pentamethylcyclopentadienes (pentaMCP) or their isomers.

substituted cyclopentadienes (m/z = 94, 108) for ZSM-22, and 3 and 4 methyl-substituted cyclopentadienes (m/z = 108, 122) for ZSM-35, are the respective main deprotonated products of methylcyclopentenyl cations.

As mentioned above, for the zeolite with the one-dimensional 10-membered ring channel, ZSM-22, the space limits the generation of polymethyl-substituted cyclopentadienes and just dimethylcyclopentadiene and trimethylcyclopentadiene can be formed. However, for two-dimensional ZSM-35 and three-dimensional ZSM-5, the spaces of the channel intersections are large enough for the generation of some bulky intermediates, such as tetramethylcyclopentadienes and pentamethylcyclopentadienes. As for the

beta zeolite investigated in our previous study, its intersections of channels of 12-membered rings can accommodate nearly any 5-membered or 6-membered, cyclic organic species. Therefore, the retained species are mostly penta- or tetramethylcyclopenta-dienes.[42] Thus, it can be seen that the number of substitution groups of cyclopentenyl cations is sensitively related to the fine structure of the zeolite, and even a little discrepancy in the channel or channel intersection has a great influence on the size and number of substitution groups of these active cations in the MTH reaction.

3.5 Mechanisms of MTH process on 10-membered ring zeolites studied by $^{12}C/^{13}C$-methanol switch experiments

The dual-cycle mechanism for the MTH reaction on ZSM-5 was proposed in 2006.[27,28] The aromatic cycle and alkene cycle make up two parts of this mechanism and respectively refer to cyclic species, like aromatics and cyclopentadienes, and chain alkenes, like propene, butenes, pentenes and hexenes, as the active intermediates. Although there is a huge discrepancy in the catalytic performance of methanol conversion over ZSM-22 and ZSM-5, the olefins generation via the alkene cycle and aromatic cycle on ZSM-22 was still evidenced in our previous study.[43] In the present study, methylcyclopentadienes and pol-ymethylbenzenes, as the main active organic species of the aromatic cycle, have also been observed on ZSM-22 and ZSM-35 (in Section 3.4), which implies the possibility of olefin genera-tion from methanol conversion in ZSM-35 with two-dimensional interconnecting channels system through the reaction route of the aromatic cycle. On the other hand, the long chain alkenes product generation over ZSM-35, similar to that over ZSM-22, suggests that the alkene methylation and cracking route is probably predominant over ZSM-35 and ZSM-22. The participation of the retained cyclic organics in methanol conversion and dual cycle mechanism over all the three 10-membered ring zeolites are studied by $^{12}C/^{13}C$-methanol switch experiments in this section.

$^{12}C/^{13}C$-methanol switch experiments were performed to distinguish the active organic species retained in the catalysts and clarify their roles in olefin generation from methanol conversion. The total ^{13}C contents of the effluent alkenes and trapped cyclic organic materials after $^{12}C/^{13}C$-methanol switch experiments are shown in Fig. 6. The differences in isotopic distribution of ^{13}C atoms in alkene products and retained compounds are distinguished among the three zeolite catalysts. Usually, the higher ^{13}C content an organic species has, the higher reactivity and greater participation the organic species exhibits.

The retained organic species displayed different ^{13}C contents, as shown in Fig. 6. On ZSM-22, the ^{13}C contents of diMCP, triMCP, tetraMCP and pentaMCP are 13%, 8.1%, 7.7% and 7.4% respectively. For ZSM-35, the respective ^{13}C contents of diMCP, triMCP, tetraMCP and pentaMCP are 15%, 13%, 11% and 7.3%. The ^{13}C contents after $^{12}C/^{13}C$-methanol switch experiments over ZSM-22 and ZSM-35 are much lower than that over ZSM-5 with the ^{13}C contents of 30%, 64%, 60% and 63% for diMCP, triMCP, tetraMCP and pentaMCP. This indicates that
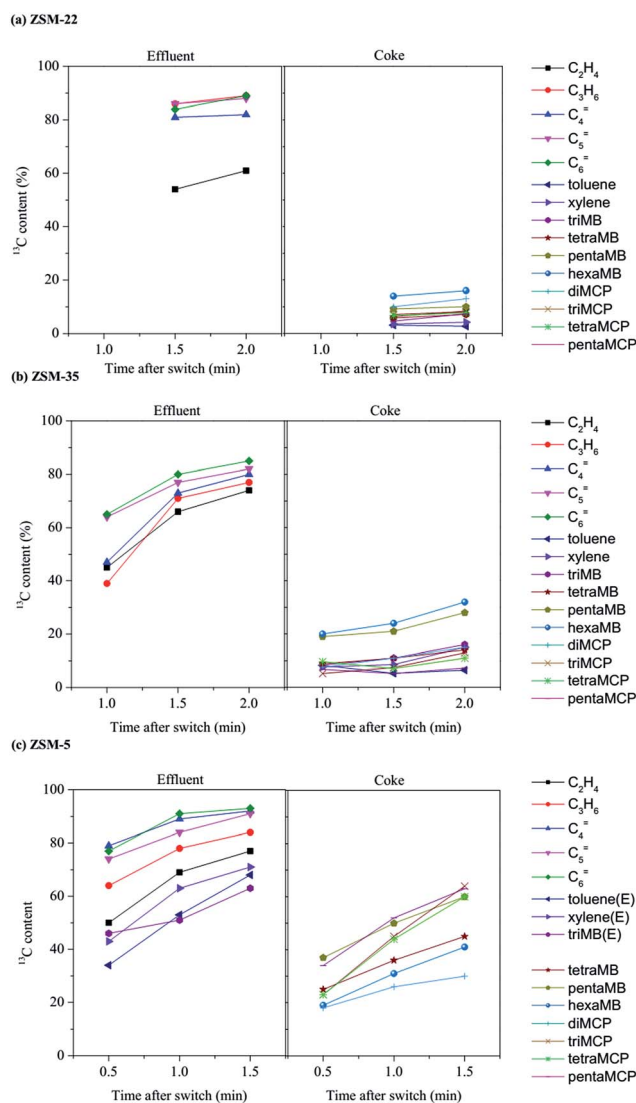

Fig. 6 ^{13}C contents of effluents and retained species in $^{12}C/^{13}C$-methanol switch experiments on ZSM-22, ZSM-35 and ZSM-5 after methanol conversion for 20 min at the reaction temperature of 300 °C and methanol WHSV of 2 h^{-1}.

the formation and participation of the MCP species over ZSM-5 are quite different from that of ZSM-22 and ZSM-35. The confinement effect of the zeolite not only affects the formation of these cyclic organics, but also varies the activity of the MCP species over different zeolites. Over ZSM-5, the predominant ^{13}C atoms incorporation into triMCP, tetraMCP and pentaMCP implied their involvement in the methanol conversion. For ZSM-22 and ZSM-35, although low ^{13}C contents of MCP species are presented, diMCP is more reactive when in contact with methanol than other MCP species with more methyl substitution.

The variation in the ^{13}C contents of the retained organic species over the three zeolites, and more importantly, the results of the $^{12}C/^{13}C$-methanol switch experiments, shown in Fig. 6, displayed the difference in the incorporation of ^{13}C atoms from the ^{13}C-methanol feed in the effluent products and

the retained organics in the catalysts. Over ZSM-22, the ^{13}C content of the effluent products, propene, butene, pentene and hexene is about 80–90% and the ^{13}C content of ethene is about 60%. However, the ^{13}C content of the retained organics over ZSM-22, such as aromatics and cyclopentadienes, is lower than 20%. On ZSM-35, ^{13}C contents of the effluent and the retained species are about 60–80% and 10–20%, respectively. The ^{13}C content gap between effluent alkenes and retained organics over ZSM-35 is still remarkable, though a little narrower than ZSM-22. The huge gap of ^{13}C content between effluents and retained species over ZSM-22 and ZSM-35 states that the methanol conversion were more closely related to the reaction route *via* the alkene cycle, and the retained organics do not play important roles. As for ZSM-5, the ^{13}C content of the retained species is about 50% for some relatively active species, far beyond those on ZSM-22 and ZSM-35, and the relatively close incorporation of ^{13}C atoms in the effluent alkenes and the retained species indicates the participation of the retained organics in the formation of alkene products.

The results of ^{12}C/^{13}C-methanol switch experiments depict that the retained species in ZSM-22 and ZSM-35 played very limited roles in the methanol conversion and olefin generation in the MTH process. Referring to the topology structure of ZSM-22, the space provided by the one-dimensioned 10-membered ring channels is not large enough for the reaction route *via* the aromatic cycle, with the participation of active and bulky cyclic species. The high incorporation of ^{13}C atoms of the alkene products indicated that the alkene cycle, based on the alkene species, proceeds in the one-dimensional channel of ZSM-22. For ZSM-35 and ZSM-5, the intersectional 2-dimensional and 3-dimensional channels provide a more spacious environment than the one-dimensional channel of ZSM-22, where bulky cyclic species like tetramethylbenzenes and pentamethylbenzene can be generated. However, in ZSM-35, even though some methylcyclopentadienes and polymethylbenzenes have been detected in the retained species in zeolites, ^{12}C/^{13}C-methanol switch experiments still demonstrated similar results to ZSM-22. The low participation of retained species in the MTH reaction implies that their function as the hydrocarbon-pool species may require a much wider environment. However, for ZSM-5, the three-dimensional intercrossing structure of all 10-membered ring channels not only ensures the space for the bulky cyclic species formation and function, but also favors the effective removal of products, which avoids the secondary reaction of the active species, such as alkenes and aromatics, and greatly suppresses the deactivation. The retained species related to the aromatic cycle in ZSM-5 all reflected high ^{13}C contents and high degrees of participation in methanol conversion and olefin production.

The aromatic cycle mechanism is based on the generation and function of bulky 5-membered and 6-membered cycle species and depends strongly on the space provided by the zeolites. The limited space in ZSM-22 seriously restricted the formation of bulky cycle species. Even though a certain number of aromatics and cyclopentadienes can be generated in ZSM-22, their relatively low ^{13}C contents suggested that they were not as active as those on ZSM-5 under the reaction conditions. The

structure of one-dimensional channels greatly suppresses the participation of cyclic species in the reaction, and methanol conversion mainly relied on the reaction route of alkene methylation and the cracking route. Due to the cracking reaction not being favorable at low temperature, a very small proportion of methanol feed is converted at the relatively low reaction temperature of 300 °C. As for ZSM-35, the intersection of 8-membered and 10-membered ring channels provides a relatively large space for the generation of intermediates required in the aromatic cycle, and more involvement of the cyclic organics can be observed through the ^{12}C/^{13}C-methanol switch experiments than that on ZSM-22. However, compared to the alkene products, the already generated cyclic species can only display weak MTO reactivity, and the alkene cycle is the predominant route for the reaction over ZSM-35. For ZSM-5, the 3-dimensional intersectional 10-membered ring structure not only affords the space for the generation of bulky species and the reaction *via* the aromatic cycle, but also improves the diffusion of olefin and aromatic products. At the same time, the improved alkene generation benefits from the abundant cyclic organics formation and will in turn promote methanol conversion to hydrocarbon products, according to the auto-catalysis of this reaction.[53,74,78–80] The mutual promotion significantly contributes to the extremely high reactivity of the MTH process over ZSM-5 than that on ZSM-22 and ZSM-35. The comparison studies of three 10-membered ring zeolites clearly depict that the slight channel differences among the three 10-membered ring zeolites vary the emphasis of the reaction route in the dual cycle mechanism and present the particularity of product generation over each zeolite catalyst.

4. Conclusions

10-Membered ring zeolites with different topologies, ZSM-22, ZSM-35 and ZSM-5, were employed as the catalysts of the methanol reaction, and the catalytic performances showed great differences in conversion and product selectivity, which were correlated to the formation of retained organic species in the MTH reaction. Further study of the ^{13}C MAS NMR and GC-MS analysis of the retained materials in the zeolites indicated that cyclopentadienes and aromatic species were generated and played important roles during the MTH reaction. The chemical environments of the three 10-membered ring zeolites apparently limit the size and structure of the retained cyclic species formed in the zeolites. During methanol conversion on ZSM-5, cyclopentadiene with 3, 4 and 5 substituted methyl groups are mainly formed as active organic species, while 2 and 3 methyl substituted cyclopentadienes for ZSM-22 and 3 and 4 methyl substituted cyclopentadienes for ZSM-35 are the respective main deprotonated products of methylcyclopentenyl cations.

The reaction routes for the dual-cycle mechanism in the methanol reaction over ZSM-22, ZSM-35 and ZSM-5 present different emphases. For ZSM-22 and ZSM-35, the reaction route, according to the aromatic cycle, is severely suppressed. The alkene cycle turns out to be the predominant route for methanol conversion. As for ZSM-5, three-dimensional intersectional channels ensure the large generation and high reactivity of

retained cyclic species, and also promote the efficient diffusion of hydrocarbon products and suppress the deactivation as well. The mutual promotion of the reaction *via* the routes of the aromatic cycle and alkene cycle significantly contributes to the excellent reactivity of ZSM-5 in the MTH reaction.

Acknowledgements

Notes and references

1 C. D. Chang and A. J. Silvestri, *J. Catal.*, 1977, **47**, 249–259.
2 C. D. Chang, *Catal. Rev.: Sci. Eng.*, 1984, **26**, 323–345.
3 M. Stocker, *Microporous Mesoporous Mater.*, 1999, **29**, 3–48.
4 U. Olsbye, S. Svelle, M. Bjorgen, P. Beato, T. V. W. Janssens, F. Joensen, S. Bordiga and K. P. Lillerud, *Angew. Chem., Int. Ed.*, 2012, **51**, 5810–5831.
5 Z. M. Liu and Y. Qi, *Chin. Sci. Bull.*, 2006, **21**, 406–408.
6 P. Tian, Y. X. Wei, M. Ye and Z. M. Liu, *ACS Catal.*, 2015, **5**, 1922–1938.
7 Y. Ono and T. Mori, *J. Chem. Soc., Faraday Trans. 1*, 1981, **77**, 2209–2221.
8 G. J. Hutchings, F. Gottschalk, M. V. M. Hall and R. Hunter, *J. Chem. Soc., Faraday Trans. 1*, 1987, **83**, 571–583.
9 G. A. Olah, *Pure Appl. Chem.*, 1981, **53**, 201–207.
10 D. Kagi, *J. Catal.*, 1981, **69**, 242–243.
11 C. D. Chang, *J. Catal.*, 1981, **69**, 244–245.
12 J. F. Haw, W. G. Song, D. M. Marcus and J. B. Nicholas, *Acc. Chem. Res.*, 2003, **36**, 317–326.
13 D. Lesthaeghe, V. Van Speybroeck, G. B. Marin and M. Waroquier, *Angew. Chem., Int. Ed.*, 2006, **45**, 1714–1719.
14 D. M. Marcus, K. A. McLachlan, M. A. Wildman, J. O. Ehresmann, P. W. Kletnieks and J. F. Haw, *Angew. Chem., Int. Ed.*, 2006, **45**, 3133–3136.
15 I. M. Dahl and S. Kolboe, *Catal. Lett.*, 1993, **20**, 329–336.
16 I. M. Dahl and S. Kolboe, *J. Catal.*, 1994, **149**, 458–464.
17 I. M. Dahl and S. Kolboe, *J. Catal.*, 1996, **161**, 304–309.
18 K. Hemelsoet, J. V. d. Mynsbrugge, K. D. Wispelaere, M. Waroquier and V. V. Speybroeck, *ChemPhysChem*, 2013, **14**, 1526–1545.
19 H. Koempel and W. Liebner, *Stud. Surf. Sci. Catal.*, 2007, **167**, 261–267.
20 J. F. Haw, J. B. Nicholas, W. G. Song, F. Deng, Z. K. Wang, T. Xu and C. S. Heneghan, *J. Am. Chem. Soc.*, 2000, **122**, 4763–4775.
21 M. Hunger and T. Horvath, *J. Am. Chem. Soc.*, 1996, **118**, 12302–12308.
22 P. W. Goguen, T. Xu, D. H. Barich, T. W. Skloss, W. G. Song, Z. K. Wang, J. B. Nicholas and J. F. Haw, *J. Am. Chem. Soc.*, 1998, **120**, 2650–2651.
23 M. Seiler, U. Schenk and M. Hunger, *Catal. Lett.*, 1999, **62**, 139–145.

24 W. G. Song, D. M. Marcus, H. Fu, J. O. Ehresmann and J. F. Haw, *J. Am. Chem. Soc.*, 2002, **124**, 3844–3845.
25 M. Seiler, W. Wang, A. Buchholz and M. Hunger, *Catal. Lett.*, 2003, **88**, 187–191.
26 M. Seiler, W. Wang and M. Hunger, *J. Phys. Chem. B*, 2001, **105**, 8143–8148.
27 S. Svelle, F. Joensen, J. Nerlov, U. Olsbye, K.-P. Lillerud, S. Kolboe and M. Bjorgen, *J. Am. Chem. Soc.*, 2006, **128**, 14770–14771.
28 M. Bjorgen, S. Svelle, F. Joensen, J. Nerlov, S. Kolboe, F. Bonino, L. Palumbo, S. Bordiga and U. Olsbye, *J. Catal.*, 2007, **249**, 195–207.
29 J. Li, Y. Qi, L. Xu, G. Liu, S. Meng, B. Li, M. Li and Z. Liu, *Catal. Commun.*, 2008, **9**, 2515–2519.
30 M. Bjorgen, F. Joensen, K. P. Lillerud, U. Olsbye and S. Svelle, *Catal. Today*, 2009, **142**, 90–97.
31 M. Bjorgen, K. P. Lillerud, U. Olsbye and S. Svelle, *Natural Gas Conversion Viii, Proceedings of the 8th Natural Gas Conversion Symposium*, 2010, vol. 167, pp. 463–468.
32 C. M. Wang, Y. D. Wang and Z. K. Xie, *Catal. Sci. Technol.*, 2014, **4**, 2631–2638.
33 X. Wang, W. L. Dai, G. J. Wu, L. D. Li, N. J. Guan and M. Hunger, *Catal. Sci. Technol.*, 2014, **4**, 688–696.
34 J. R. Chen, J. Z. Li, C. Y. Yuan, S. T. Xu, Y. X. Wei, Q. Y. Wang, Y. Zhou, J. B. Wang, M. Z. Zhang, Y. L. He, S. L. Xu and Z. Liu, *Catal. Sci. Technol.*, 2014, **4**, 3268–3277.
35 X. Y. Sun, S. Mueller, H. Shi, G. L. Haller, M. Sanchez-Sanchez, A. C. van Veen and J. A. Lercher, *J. Catal.*, 2014, **314**, 21–31.
36 X. Y. Sun, S. Mueller, Y. Liu, H. Shi, G. L. Haller, M. Sanchez-Sanchez, A. C. van Veen and J. A. Lercher, *J. Catal.*, 2014, **317**, 185–197.
37 W. G. Song, J. B. Nicholas, A. Sassi and J. F. Haw, *Catal. Lett.*, 2002, **81**, 49–53.
38 W. G. Song, J. B. Nicholas and J. F. Haw, *J. Phys. Chem. B*, 2001, **105**, 4317–4323.
39 T. Xu, D. H. Barich, P. W. Goguen, W. G. Song, Z. K. Wang, J. B. Nicholas and J. F. Haw, *J. Am. Chem. Soc.*, 1998, **120**, 4025–4026.
40 J. F. Haw, P. W. Goguen, T. Xu, T. W. Skloss, W. G. Song and Z. K. Wang, *Angew. Chem., Int. Ed.*, 1998, **37**, 948–949.
41 S. T. Xu, A. M. Zheng, Y. X. Wei, J. R. Chen, J. Z. Li, Y. Y. Chu, M. Z. Zhang, Q. Y. Wang, Y. Zhou, J. B. Wang, F. Deng and Z. M. Liu, *Angew. Chem., Int. Ed.*, 2013, **52**, 11564–11568.
42 M. Z. Zhang, S. T. Xu, J. Z. Li, Y. X. Wei, Y. J. Gong, Y. Y. Chu, A. M. Zheng, J. B. Wang, W. N. Zhang, X. Q. Wu, F. Deng and Z. M. Liu, *J. Catal.*, 2016, **335**, 47–57.
43 J. B. Wang, Y. X. Wei, J. Z. Li, S. T. Xu, W. N. Zhang, Y. L. He, J. R. Chen, M. Z. Zhang, A. M. Zheng, F. Deng, X. W. Guo and Z. M. Liu, *Catal. Sci. Technol.*, 2016, **6**, 89–97.
44 C. Wang, Y. Y. Chu, A. M. Zheng, J. Xu, Q. Wang, P. Gao, G. D. Qi, Y. J. Gong and F. Deng, *Chem.–Eur. J.*, 2014, **20**, 12432–12443.
45 C. Wang, X. F. Yi, J. Xu, G. D. Qi, P. Gao, W. Y. Wang, Y. Y. Chu, Q. Wang, N. D. Feng, X. L. Liu, A. M. Zheng and F. Deng, *Chem.–Eur. J.*, 2015, **21**, 12061–12068.

46 C. Wang, J. Xu, G. D. Qi, Y. J. Gong, W. Y. Wang, P. Gao, Q. Wang, N. D. Feng, X. L. Liu and F. Deng, *J. Catal.*, 2015, **332**, 127–137.

47 C. Wang, Q. Wang, J. Xu, G. D. Qi, P. Gao, W. Y. Wang, Y. Y. Zou, N. D. Feng, X. L. Liu and F. Deng, *Angew. Chem., Int. Ed.*, 2016, **55**, 2507–2511.

48 J. Z. Li, Y. X. Wei, J. R. Chen, P. Tian, X. Su, S. T. Xu, Y. Qi, Q. Y. Wang, Y. Zhou, Y. L. He and Z. M. Liu, *J. Am. Chem. Soc.*, 2012, **134**, 836–839.

49 J. Z. Li, Y. X. Wei, J. R. Chen, S. T. Xu, P. Tian, X. F. Yang, B. Li, J. B. Wang and Z. M. Liu, *ACS Catal.*, 2015, **5**, 661–665.

50 S. Teketel, M. W. Erichsen, F. L. Bleken, S. Svelle and K. Petter, *Spec. Period. Rep.: Catal.*, 2014, **26**, 179–217.

51 J. R. Chen, J. Z. Li, Y. X. Wei, C. Y. Yuan, B. Li, S. T. Xu, Y. Zhou, J. B. Wang, M. Z. Zhang and Z. M. Liu, *Catal. Commun.*, 2014, **46**, 36–40.

52 S. Teketel, W. Skistad, S. Benard, U. Olsbye, K. P. Lillerud, P. Beato and S. Svelle, *ACS Catal.*, 2012, **2**, 26–37.

53 J. Z. Li, Y. X. Wei, G. Y. Liu, Y. Qi, P. Tian, B. Li, Y. L. He and Z. M. Liu, *Catal. Today*, 2011, **171**, 221–228.

54 W. L. Dai, X. Wang, G. J. Wu, N. J. Guan, M. Hunger and L. D. Li, *ACS Catal.*, 2011, **1**, 292–299.

55 W. L. Dai, M. Scheibe, N. J. Guan, L. D. Li and M. Hunger, *ChemCatChem*, 2011, **3**, 1130–1133.

56 W. L. Dai, C. M. Wang, M. Dyballa, G. J. Wu, N. J. Guan, L. D. Li, Z. K. Xie and M. Hunger, *ACS Catal.*, 2015, **5**, 317–326.

57 M. Bjørgen, U. Olsbye, D. Petersen and S. Kolboe, *J. Catal.*, 2004, **221**, 1–10.

58 Q. Wang, Z. M. Cui, C. Y. Cao and W. G. Song, *J. Phys. Chem. C*, 2011, **115**, 24987–24992.

59 Y. Y. Chu, X. Y. Sun, X. F. Yi, L. H. Ding, A. M. Zheng and F. Deng, *Catal. Sci. Technol.*, 2015, **5**, 3507–3517.

60 S. Teketel, L. F. Lundegaard, W. Skistad, S. M. Chavan, U. Olsbye, K. P. Lillerud, P. Beato and S. Svelle, *J. Catal.*, 2015, **327**, 22–32.

61 J. Z. Li, Y. X. Wei, Y. Qi, P. Tian, B. Li, Y. L. He, F. X. Chang, X. D. Sun and Z. M. Liu, *Catal. Today*, 2011, **164**, 288–292.

62 F. F. Wei, Z. M. Cui, X. J. Meng, C. Y. Cao, F. S. Xiao and W. G. Song, *ACS Catal.*, 2014, **4**, 529–534.

63 S. C. Baek, Y. J. Lee, K. W. Jun and S. B. Hong, *Energy Fuels*, 2009, **23**, 593–598.

64 G. T. Kokotailo, J. L. Schlenker, F. G. Dwyer and E. W. Valyocsik, *Zeolites*, 1985, **5**, 349–351.

65 J. B. Wang, J. Z. Li, S. T. Xu, Y. C. Zhi, Y. X. Wei, Y. L. He, J. R. Chen, M. Z. Zhang, Q. Y. Wang, W. N. Zhang, X. Q. Wu, X. W. Guo and Z. M. Liu, *Chin. J. Catal.*, 2015, **36**, 1392–1402.

66 J. B. Wang, S. T. Xu, J. Z. Li, Y. C. Zhi, M. Z. Zhang, Y. L. He, Y. X. Wei, X. W. Guo and Z. M. Liu, *RSC Adv.*, 2015, **5**, 88928–88935.

67 S. J. Xie, J. B. Peng, L. Y. Xu, Z. H. Wu and Q. X. Wang, *Chin. J. Catal.*, 2003, **24**, 531–534.

68 Y. Liu, W. P. Zhang, S. J. Xie, L. Y. Xu, X. W. Han and X. H. Bao, *J. Phys. Chem. B*, 2008, **112**, 1226–1231.

69 Y. Y. Yuan, L. Y. Wang, H. C. Liu, P. Tian, M. Yang, S. T. Xu and Z. M. Liu, *Chin. J. Catal.*, 2015, **36**, 1910–1919.

70 D. Massiot, F. Fayon, M. Capron, I. King, S. Le Calvé, B. Alonso, J.-O. Durand, B. Bujoli, Z. H. Gan and G. Hoatson, *Magn. Reson. Chem.*, 2002, **40**, 70–76.

71 M. Guisnet, *J. Mol. Catal. A: Chem.*, 2002, **182**, 367–382.

72 W. Loewenstein, *Am. Mineral.*, 1954, **39**, 92–96.

73 D. M. McCann, D. Lesthaeghe, P. W. Kletnieks, D. R. Guenther, M. J. Hayman, V. Van Speybroeck, M. Waroquier and J. F. Haw, *Angew. Chem., Int. Ed.*, 2008, **47**, 5179–5182.

74 N. Y. Chen and W. J. Reagan, *J. Catal.*, 1979, **59**, 123–129.

75 W. P. Zhang, S. T. Xu, X. W. Han and X. H. Bao, *Chem. Soc. Rev.*, 2012, **41**, 192–210.

76 A. M. Zheng, S. B. Liu and F. Deng, *Acc. Chem. Res.*, 2016, **49**, 655–663.

77 A. M. Zheng, S. J. Huang, S. B. Liu and F. Deng, *Phys. Chem. Chem. Phys.*, 2011, **13**, 14889–14901.

78 S. Ilias and A. Bhan, *J. Catal.*, 2012, **290**, 186–192.

79 S. Ilias and A. Bhan, *ACS Catal.*, 2013, **3**, 18–31.

80 S. Ilias, R. Khare, A. Malek and A. Bhan, *J. Catal.*, 2013, **303**, 135–140.